Reversible Thermal Denaturation of Human FGF-1 Induced by Low Concentrations of Guanidine Hydrochloride

Sachiko I. Blaber,* Juan F. Culajay,* Archana Khurana,* and Michael Blaber*#
*Institute of Molecular Biophysics and #Department of Chemistry, Florida State University, Tallahassee, Florida 32306-4380 USA

ABSTRACT Human acidic fibroblast growth factor (FGF-1) is a powerful mitogen and angiogenic factor with an apparent melting temperature (T_m) in the physiological range. FGF-1 is an example of a protein that is regulated, in part, by stability-based mechanisms. For example, the low T_m of FGF-1 has been postulated to play an important role in the unusual endoplasmic reticulum-independent secretion of this growth factor. Despite the close relationship between function and stability, accurate thermodynamic parameters of unfolding for FGF-1 have been unavailable, presumably due to effects of irreversible thermal denaturation. Here we report the determination of thermodynamic parameters of unfolding (ΔH, ΔG, and ΔC_p) for FGF-1 using differential scanning calorimetry (DSC). The thermal denaturation is demonstrated to be two-state and reversible upon the addition of low concentrations of added guanidine hydrochloride (GuHCl). ΔG values from the DSC studies are in excellent agreement with values from isothermal GuHCl denaturation monitored by fluorescence and circular dichroism (CD) spectroscopy. Furthermore, the results indicate that irreversible denaturation is closely associated with the formation of an unfolding intermediate. GuHCl appears to promote reversible two-state denaturation by initially preventing aggregation of this unfolding intermediate, and at subsequently higher concentrations, by preventing formation of the intermediate.

INTRODUCTION

Human acidic fibroblast growth factor (FGF-1) is a member of a family of mitogens and hormones whose diverse action is mediated through tyrosine kinase receptors (Bourque et al., 1993; Mellin et al., 1992; Fitzpatrick et al., 1992; Ortega et al., 1998; Deng et al., 1996; Colvin et al., 1996; Slack et al., 1987). Various members of the FGF family are potent angiogenic factors (Thomas et al., 1985; Thompson et al., 1989; Schneider and Parker, 1991; Yanagisawa-Miwa et al., 1992), with potential use in "angiogenic therapy" to treat ischemia (Landau et al., 1995; Unger et al., 1994; Yanagisawa-Miwa et al., 1992; Pu et al., 1993; Thompson et al., 1989; Nabel et al., 1993; Schlaudraff et al., 1993; Schumacher et al., 1998). These growth factors are also termed "heparin binding" growth factors due to their specific affinity for this polysulfonated polysaccharide. Early characterization of FGF-1 indicated that binding of heparin could protect the protein from denaturation by acid, proteolysis, and mild oxidation (Gospodarowicz and Cheng, 1986; Rosengart et al., 1988; Linemeyer et al., 1990). Differential scanning calorimetry (DSC) by Middaugh and coworkers (Copeland et al., 1991) suggested that the melting temperature (T_m) of FGF-1 is close to physiological. However, other thermodynamic parameters (i.e., ΔH, ΔG, or ΔC_p) were not reported, presumably due to irreversible denaturation. The interaction of FGF-1 with heparin was reported by this group to increase the T_m by ~20 K. This provided a rationale for the protection of FGF-1 by heparin against thermal denaturation and proteolysis. The low T_m of FGF-1 seems a paradox: why would a protein have a thermal stability that results in a significant population of molecules being unfolded (and therefore inactive) in the temperature regime within which they are intended to function?

The thermal stability of FGF-1 may provide an important regulatory mechanism with regard to membrane translocation and cell secretion. FGF-1, like basic FGF (FGF-2), lacks a characteristic secretion signal sequence (Abraham et al., 1986; Jaye et al., 1986) and is secreted by an endoplasmic reticulum-independent mechanism. Cytosolic FGF-1 is secreted in response to heat shock, and appears to have a different conformation from the native protein (Jackson et al., 1992). A fusion protein of FGF-1 and diphtheria toxin has been reported to translocate across the cytosolic membrane, but only under low pH conditions and not if FGF-1 is stabilized by binding sulfate ion or sulfonated molecules (Wiedlocha et al., 1992). FGF-1 has subsequently been shown to form partially structured states under such acidic conditions (Mach et al., 1993; Sanz and Gimenez-Gallego, 1997). Furthermore, these partially structured states can interact with negatively charged phospholipid vesicles, contributing to disruption of such vesicles (Mach and Middaugh, 1995). Thus, the low thermal stability of FGF-1 may be related to the ability to form partially structured states at physiological temperatures that can directly translocate across cellular membranes (Bychkova et al., 1988). In the case of secretion, once outside the cell, binding to heparin in the extracellular matrix or heparan sulfate on the surface of cells, can stabilize FGF-1. Therefore, modulation of the stability of FGF-1 is an essential aspect of its regulation and function.

Received for publication 7 January 1999 and in final form 6 April 1999.

Address reprint requests to Dr. Michael Blaber, Institute of Molecular Biophysics, 104 MBB-4380, Florida State University, Tallahassee, FL 32306-4380. Tel.: 850-644-5870; Fax: 850-561-1406; E-mail: blaber@sb.fsu.edu.

0006-3495/99/07/470/08 $2.00

Despite the importance of stability to the function of FGF-1, detailed thermodynamic parameters of unfolding have not been available. Here we report the use of low concentrations of guanidine hydrochloride (GuHCl) to prevent aggregation during thermal denaturation of FGF-1, thus allowing the determination of thermodynamic parameters of unfolding (ΔH, T_m, and ΔC_p). The data are compared to GuHCl-induced unfolding under isothermal conditions using a combination of fluorescence and circular dichroism (CD) spectroscopy. The results from the different methods are in excellent agreement. The analysis elucidates the role of an unfolding intermediate in the thermal aggregation of FGF-1 and the role of GuHCl in promoting two-state thermal denaturation.

MATERIALS AND METHODS

The choice of buffer with which to perform DSC, CD, and fluorescent studies was of primary concern. DSC analysis requires a buffer with a low ionization enthalpy, while the spectroscopic studies require buffers that will not absorb significantly over the wavelength of interest. Furthermore, thermodynamic data are of greatest value when collected under conditions similar to those used for other structural and functional studies. Since the crystal structure of FGF was solved at pH 6.2 (Blaber et al., 1996) and biological assays are performed near pH 7.4, a buffer with a pK_a in this region was desirable. Although phosphate buffer is an excellent choice for DSC studies due to its low ionization enthalpy, crystallographic studies have demonstrated that FGF-1 will bind phosphate ions (Romero et al., 1996). Furthermore, this binding site in FGF-1 can also bind sulfate ions (Blaber et al., 1996), thus sulfonic acid-based buffers can also potentially bind to FGF-1. Binding of such ions by FGF-1 can increase the protein stability (Blaber et al., 1997). Although *N*-(2-acetamido)iminodiacetic acid (ADA; $pK_a = 6.60$) can interfere with CD measurements below 210 nm, it is a good compromise for overall use in the DSC, CD, and fluorescence studies.

Protein preparation

A synthetic gene for the 140 amino acid form of human acidic fibroblast growth factor (Gimenez-Gallego et al., 1986; Linemeyer et al., 1987) was inserted into the PET-21 vector (Novagen, Inc., Madison, WI) and introduced into *Escherichia coli* strain BL21(DE3). The transformed *E. coli* was grown at 37°C in M9 minimal media (Sambrook et al., 1989) to an optical density of $A_{600} = 1.5$, at which point the temperature was shifted to 28°C and expression of FGF was induced by the addition of 1 mM isopropyl β-D-thiogalactopyranoside (IPTG). The cells were allowed to grow for an additional 3.0 h and were then harvested by centrifugation (5,000 × *g* for 10 min). The cell paste was stored frozen at −20°C before use. Purification to apparent homogeneity on Coomassie Brilliant Blue-stained sodium dodecyl sulfate (SDS) gels was accomplished using a combination of Carboxymethyl- and Sulphopropyl-Sephadex ion exchange resins, followed by Sephadex G-50 gel filtration chromatography and heparin-Sepharose affinity chromatography (all resins from Pharmacia, Piscataway, NJ). Details of the purification procedure will be provided elsewhere. The purified protein was concentrated to 1.2 mg/ml using a pressure cell and YM-10 membrane (Amicon, Beverly, MA) and dialyzed versus three 1:100 vol/vol changes of 20 mM *N*-(2-acetamido)iminodiacetic acid (ADA), 0.1 M NaCl pH 6.60 ("ADA buffer") using Spectrapore 1 (6–8 kDa cutoff) dialysis tubing (Spectrum Industries, Houston, TX). The dialyzed protein was filtered using a 0.2 μm syringe filter (Gellman Sciences, Ann Arbor, MI) and diluted to 1.0 mg/ml with ADA buffer. The protein sample was then aliquoted and stored frozen at −80°C before use. Protein concentrations were determined using an extinction coefficient E (0.1%, 1 cm) = 1.26 at 280 nm and a molecular mass of 15.9 kDa (Zazo et al., 1992; Tsai et al., 1993). For studies involving the addition of GuHCl a stock solution of 8 M GuHCl in ADA buffer was made by addition of GuHCl (Heico Chemical, Delaware Water Gap, PA) to ADA buffer, followed by 0.2 μm filtration. The final concentration of GuHCl in this stock solution was determined by refractive index measurement (Shirley, 1995). Thawed protein samples were filtered using a 0.2 μm syringe filter (Gelman Sciences), and diluted in filtered ADA buffer or GuHCl/ADA buffer to a final concentration of 0.038 mM for all studies.

DSC

DSC analyses were performed using a model VP-DSC microcalorimeter (MicroCal, Inc., Northampton, MA). All samples were degassed for 15 min prior to loading, and analyses were performed under 35 psi nitrogen gas. Unless otherwise indicated, all studies were performed by scanning from low to high temperature ("upscans") at 15 K/h. In all cases, a series of repetitive buffer/buffer scans were run and after establishing a repeatable buffer/buffer baseline, protein samples were introduced at 298 K during the cooling phase preceding the next scan cycle. In this way repetitive protein scans were collected with minimal thermal disruption and without interrupting the scan cycle. Data from the second protein run were typically the most reproducible, and these data were used for analysis. Each experiment was repeated and data from duplicate experiments were averaged.

Analysis of the DSC data was performed using both a statistical mechanics-based deconvolution (Freire and Biltonen, 1978; Kidokoro and Wada, 1987) as implemented in the *DDCL1* software package (Kidokoro and Wada, 1987; Kidokoro et al., 1988; Nakagawa and Oyanagi, 1980), and a nonlinear least-squares fit to a two-state model (Kidokoro and Wada, 1987; Kidokoro et al., 1988) using the general-purpose nonlinear fitting program *DataFit* (Oakdale Engineering, Oakdale, PA). The two-state model utilized is as follows:

$$C_p(T) = C_N(T) + \Delta C_p(T) \cdot (1 - F_N(T)) + \left(\frac{\Delta H(T)^2 \cdot F_N(T) \cdot (1 - F_N(T))}{RT^2} \right)$$

where $C_N(T)$ is the linear heat capacity function of the native state, $\Delta C_p(T)$ is the temperature-dependent difference heat capacity function between the native and denatured states, $F_N(T)$ is the temperature-dependent native state fractional component, and $\Delta H(T)$ is the temperature-dependent enthalpy of the system. The thermodynamic parameters of unfolding were determined from the nonlinear fit to the two-state model. Deviation from two-state behavior was determined by comparing van't Hoff and calorimetric enthalpies from the deconvolution analysis, the fractional component of intermediate states as determined by the deconvolution analysis, and by the error associated with the nonlinear fit to a two-state function. For the DSC data, ΔG as a function of temperature was calculated as follows:

$$\Delta G(T) = -DA \cdot T \cdot (T - T_m) - DB \cdot T \cdot \ln\left(\frac{T}{T_m}\right) + DC \cdot \left(1 - \frac{T}{T_m}\right)$$

where *DA*, *DB*, and *DC* are terms of the second-order polynomial function describing ΔH of unfolding and T_m is the melting temperature (Kidokoro and Wada, 1987; Kidokoro et al., 1988).

Fluorescence

Samples of FGF-1 in GuHCl/ADA buffer were allowed to equilibrate by overnight incubation at 4°C. Spectroscopic measurements were performed using a model FL1T1-Tau Fluorolog-Tau2 spectrofluorometer (ISA SPEX, Edison, NJ). Temperature control was achieved using a model RTE-3 circulating water bath (NESLAB, Portsmouth, NH). All experiments were

carried out at 298 K using a 10-mm pathlength cuvette. An excitation wavelength of 295 nm was used to preferentially excite the single tryptophan residue and to minimize excitation of the eight tyrosine residues present in FGF-1 (Gimenez-Gallego et al., 1986). Excitation and emission slits were set to 0.5 nm. Emission spectra were collected from 300 to 500 nm in 1.0-nm increments with a 0.5-s integration time. Scans were collected in triplicate for each sample, duplicate samples were analyzed, and the results averaged. For each protein sample, buffer baselines with the same concentration of GuHCl concentration were subtracted from the averaged protein scan. The total fluorescence from 300 to 500 nm was determined by integration of these buffer-subtracted protein scans. The fluorescence data were analyzed using the general-purpose nonlinear fitting program *DataFit* (Oakdale Engineering) using a six-parameter, two-state model (Eftink, 1994):

$$F = \frac{F_0N + (S_N \cdot [D]) + (F_oD + (S_D \cdot [D])) \cdot \exp -((\Delta G_0 + (m \cdot [D]))/RT)}{1 + \exp -((\Delta G_0 + (m \cdot [D]))/RT)}$$

where the denaturant concentration is given by $[D]$, the native state (0 M denaturant) fluorescence intercept and slope are F_{0N} and S_N, respectively, the denatured state fluorescence intercept and slope are F_{0D} and S_D, respectively, and the free energy of unfolding function intercept and slope are ΔG_0 and m, respectively.

Circular dichroism

Samples of FGF-1 in GuHCl/ADA buffer were allowed to equilibrate by overnight incubation at 4°C. Circular dichroism measurements were carried out with a model 62A DS circular dichroism spectrometer (AVIV, Burlington, MA), fitted with a thermoelectric cuvette holder, and interfaced with a model CFT-33 refrigerated recirculator (NESLAB). Isothermal (298 K) CD spectra were acquired by scanning from 260 nm down to 210 nm in 1-nm increments with a 1-nm bandwidth. A 1-mm pathlength cuvette was used to minimize the absorption effect from ADA buffer in the far UV range. Triplicate scans were recorded for each protein sample, duplicate samples were analyzed and averaged. After subtraction of buffer from protein spectra, the data were converted to molar ellipticity (deg · cm^2 · $dmol^{-1}$). A difference CD spectrum for FGF-1, comparing native and denatured states, exhibits a maximum at 227 nm. Therefore, thermal scans at fixed denaturant concentrations were performed by following the molar ellipticity at 227 nm as a function of temperature. Thermal denaturation data were collected using a scan rate of 15 K/h (identical to the DSC analysis). The CD data were analyzed using a six-parameter, two-state model as described above.

RESULTS

DSC

Initial analyses indicated that DSC data collected at the commonly used scan rate of 60 K/h were unreliable due to a hysteresis of ~4 K between upscan and downscan data. No such hysteresis is observed when the scan rate is reduced to 15 K/h (Fig. 1), the scan rate chosen for all studies. The first and second upscan of FGF-1 in various concentrations of GuHCl are shown in Fig. 2. In ADA buffer alone, the DSC trace is characterized by 1) an apparent *negative* value for ΔC_p, 2) noise in the post-transition baseline, 3) no endothermic signal on the second scan, and 4) visible precipitation after thermal denaturation (Fig. 2). These features reflect the combined effects of the denaturation endotherm, precipitation exotherm, and noise due to nonhomogenous distribution of the precipitated sample within the cell. ΔC_p values for soluble proteins are positive and typically in the range of 0.30–0.70 J g^{-1} K^{-1} (Privalov, 1979; Privalov and Potekhin, 1986) and the aberrant negative value for ΔC_p reflects the (exothermic) precipitation process.

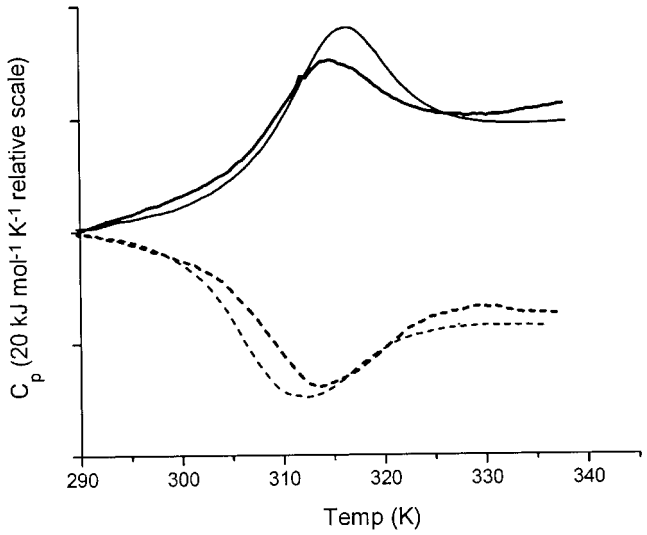

FIGURE 1 DSC endotherms (*upscans in solid lines, downscans in broken lines*) of FGF-1 at either 60 K/h (*thin lines*) or 15 K/h (*thick lines*). A hysteresis of ~4 K is observed at the 60 K/h scan rate, while no hysteresis is observed at the 15 K/h scan rate. All samples contain 0.7 M GuHCl in ADA buffer.

In an attempt to eliminate precipitation and obtain reversible thermal denaturation, the effect of added denaturant was investigated. With the addition of 0.4 M GuHCl in the ADA buffer, there was a recovery of ~16% of the denaturation enthalpy during a subsequent upscan (Fig. 2). Qualitatively, the precipitation in this sample appeared as a diffuse opacity and not an aggregation at the bottom of the sample (as observed in the ADA buffer in the absence of denaturant); however, the value for ΔC_p remained negative. At 0.5 M GuHCl, a small amount of precipitation was visible after thermal denaturation, and the recovery of calorimetric enthalpy on a subsequent scan increased to ~40% (Fig. 2). ΔC_p remained negative, however, indicating the presence of aggregation. Upon the addition of 0.6 M GuHCl there was 1) no precipitation, 2) no noise in the post-transition baseline, 3) a highly repeatable endotherm in subsequent scans, and 4) a *positive* value for ΔC_p (Fig. 2, Table 1).

Although the thermal denaturation in 0.6 M GuHCl is reversible with no precipitation, double deconvolution analysis (Kidokoro and Wada, 1987; Kidokoro et al., 1988; Nakagawa and Oyanagi, 1980) of the DSC data indicates the denaturation is non-two-state, and that an unfolding intermediate is present (Fig. 3). An unfolding intermediate is also indicated by the characteristic deviation of the observed isotherm from a nonlinear least-squares fit to a two-state model (Kidokoro and Wada, 1987; Kidokoro et al., 1988) (Fig. 4, Table 1). Additionally, the ratio of the van't Hoff to calorimetric enthalpies yields a value of 0.50

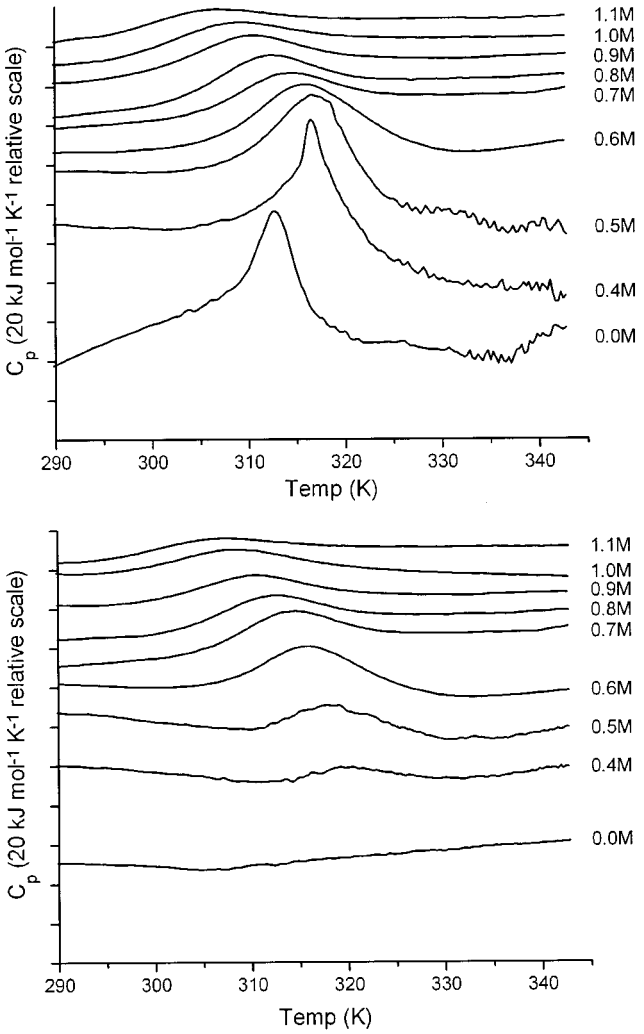

FIGURE 2 DSC endotherms for the initial (*top*) and subsequent (*bottom*) upscan of FGF-1 in concentrations of GuHCl from 0.0 to 1.1 M in ADA buffer at pH 6.60.

(Table 1), characteristic of an unfolding intermediate. With an increase in the concentration of GuHCl to 0.7 M, there is no evidence of an unfolding intermediate in the double deconvolution analysis (Fig. 3). Furthermore, there is excellent agreement of the observed isotherm with the nonlinear least-squares fit to a two-state model (Fig. 4, Table 1) and the ratio of the van't Hoff to calorimetric enthalpy is essentially 1.0 (Table 1). The root mean square (RMS) deviation between the experimental data and a two-state fit for all data between 0.7 and 1.0 M GuHCl is equivalent to the noise level of the instrument (Table 1). The data at 1.1 M GuHCl have somewhat higher error, reflecting the small enthalpic signal under these conditions. At a concentration >1.1 M GuHCl, the enthalpy decreases to the point where it is difficult to collect accurate data. Furthermore, at concentrations of GuHCl >1.1 M FGF-1 appears to be significantly unfolded even at the initial temperature of the DSC analysis. Thus, the deviation from unity of the van't Hoff/calorimetric enthalpy for the 1.1 M GuHCl sample may reflect the partially unfolded state of the sample at low temperature. Over the range of added GuHCl where two-state behavior is demonstrated (0.7–1.1 M GuHCl), ΔC_p remains relatively constant with an average value of 0.587 ± 0.036 J g^{-1} K^{-1} (Table 1). This value is less than a previously reported value of 0.74 J g^{-1} K^{-1} estimated from urea denaturation experiments performed in phosphate buffer (Burke et al., 1993).

Isothermal equilibrium denaturation: fluorescence

Isothermal equilibrium denaturation of FGF-1 by GuHCl in ADA buffer was monitored by the intrinsic fluorescence emission spectra of the single tryptophan residue in FGF-1 (Gimenez-Gallego et al., 1986; Linemeyer et al., 1987). With increasing GuHCl, there is an increase in the fluorescence emission intensity without a change in the λ_{max} (353 nm) for emission (Fig. 5). Calculation of thermodynamic constants yields an m value of -19.44 kJ L mol^{-2}, and a value for ΔG at 0M denaturant of 21.92 kJ mol^{-1} (Table 2). The midpoint of the denaturation occurs at a concentration of 1.13 M GuHCl.

Isothermal equilibrium denaturation: circular dichroism

Isothermal equilibrium denaturation monitored by changes in CD spectrum provides a more global analysis than the fluorescence spectra. The CD spectrum of FGF-1 can be measured to ~210 nm in the far UV range due to the absorbance of the ADA buffer at shorter wavelengths. Over the far UV region, the molar ellipticity of native FGF-1 exhibits a maximum at 227 nm. In response to increasing GuHCl, the molar ellipticity decreases (Fig. 5). The wavelength peak of the native spectrum (227 nm) is also the peak of the differential spectrum between native and denatured states. Calculation of thermodynamic constants yields an m value of -18.67 kJ L mol^{-2}, and a value for ΔG at 0 M denaturant of 20.76 kJ mol^{-1} (Table 2). The midpoint of the denaturation occurs at a concentration of 1.11 M GuHCl. A similar analysis using the absorbance signal at 222 nm gives essentially identical results (data not shown). Protein absorbing to the quartz cuvettes prevented thermal denaturation studies of FGF-1 using CD spectroscopy. No such absorbance was observed in the isothermal denaturant studies, using either CD or fluorescence, or thermal DSC scans (with a Tantalum cell).

DISCUSSION

DSC

Thermal denaturation of FGF-1 in the absence of GuHCl results in significant precipitation and thus is not an equilibrium process. Such endotherms cannot be deconvoluted using models that assume equilibrium. Decreasing precipitation and increasing recovery of enthalpy is demonstrated

TABLE 1 Thermodynamic parameters of unfolding for denaturation of FGF-1 in the presence of GuHCl and under equilibrium conditions

GuHC (M)	$\Delta H(T_m)$ (kJ mol^{-1})	T_m (°K)	$\Delta C_p(T_m)$ (J g^{-1} K^{-1})	2-State Fit RMS (kJ mol^{-1} K^{-1})*	$H_{van't\ Hoff}/H_{cal}$	Repeatability (%)
0.6	305.6 ± 3.4	315.7 ± 0.1	0.160 ± 0.012	1.41	0.50	85
0.7	257.3 ± 3.1	312.6 ± 0.1	0.409 ± 0.033	0.18	1.08	93
0.8	234.4 ± 3.7	310.1 ± 0.2	0.525 ± 0.043	0.12	1.04	90
0.9	197.0 ± 2.9	307.0 ± 0.2	0.621 ± 0.025	0.13	1.05	95
1.0	171.9 ± 2.5	304.8 ± 0.2	0.577 ± 0.025	0.14	1.03	83
1.1	123.1 ± 11.6	299.9 ± 0.8	0.639 ± 0.043	0.21	1.25	88

Reported error refers to the deviation from the fit to a two-state model.
*RMS deviation for the fitted function in comparison with the raw data.

with the addition of 0.4 and 0.5 M GuHCl. At concentrations of 0.6 M GuHCl and higher, there is an absence of precipitation and a recovery of essentially all the enthalpy on subsequent scans. Thus, at concentrations of 0.6 M GuHCl and higher, the two-state model can be evaluated using the equilibrium assumption. The DSC endotherm of the 0.6 M GuHCl sample is consistent with the presence of an unfolding intermediate, while at higher concentrations of denaturant there is excellent agreement with the two-state model. Although deconvolution analysis of the 0.4 and 0.5 M GuHCl data also indicates the presence of an unfolding intermediate (data not shown), the precipitation present under these conditions precludes accurate analyses of thermodynamic parameters. GuHCl may promote reversible denaturation of FGF-1 by preventing aggregation of the unfolding intermediate. At higher concentrations (0.7 M and

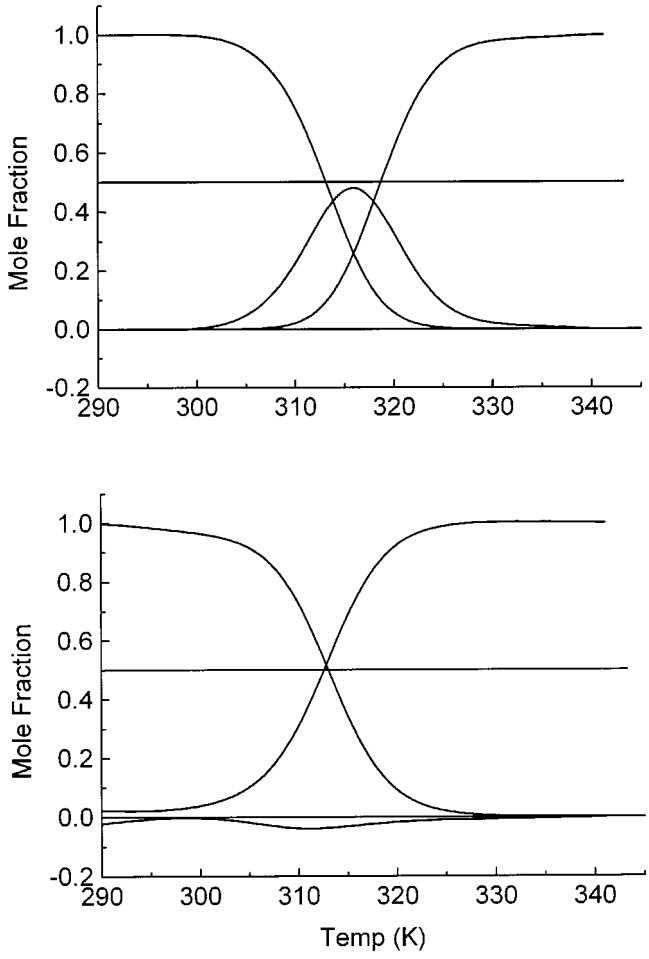

FIGURE 3 Temperature dependence of the fractional composition of native (F_N) and denatured (F_D) states of FGF-1 as determined by the double-deconvolution of the DSC data. The presence of an intermediate state is calculated by $1 - (F_N + F_D)$. Data are shown for ADA buffer with the addition of 0.6 M GuHCl (*top*), and 0.7 M GuHCl (*bottom*).

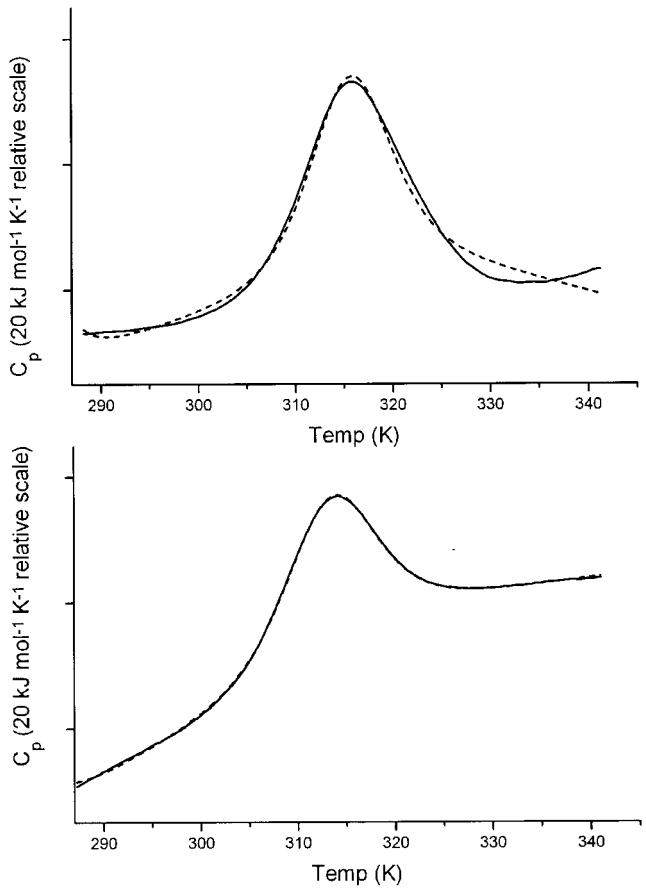

FIGURE 4 FGF-1 DSC denaturation endotherms (*solid lines*) and nonlinear least squares fit to a two-state model (Kidokoro and Wada, 1987; Kidokoro et al., 1988) (*broken lines*). The top panel shows the endotherm in the presence of 0.6 M GuHCl and the bottom panel shows the endotherm in 0.7 M GuHCl.

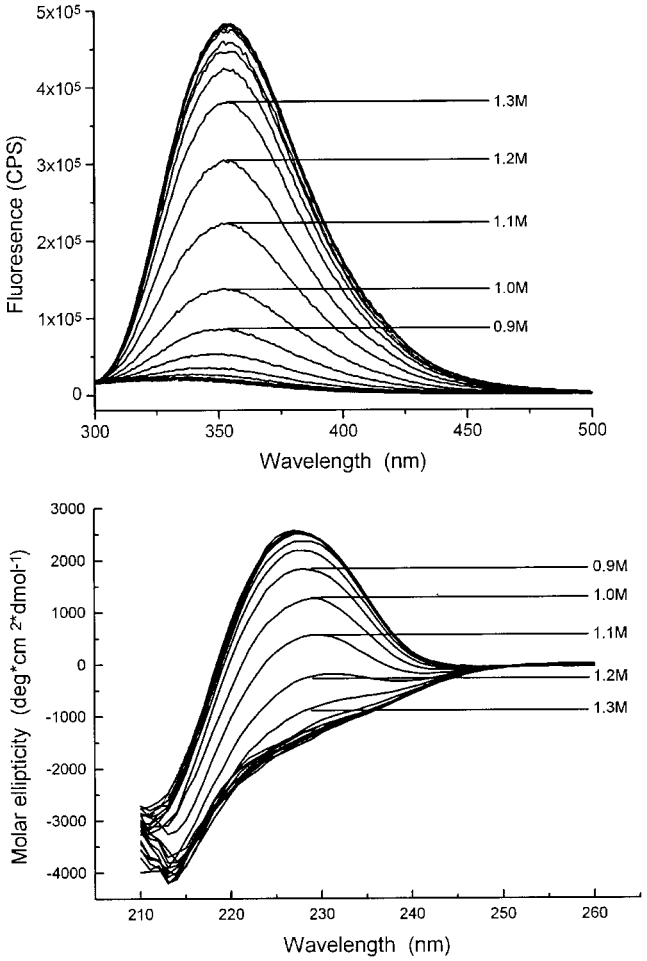

FIGURE 5 Fluorescence emission spectra of FGF-1 as a function of GuHCl (*top*). The fluorescence of FGF-1 increases with increasing GuHCl, with a characteristic maximum at 353 nm. CD spectra of FGF-1 as a function of GuHCl in the far UV range (*bottom*). The CD spectra of FGF-1 decrease over the far UV range as a function of GuHCl, with a characteristic maximum at 227 nm.

higher) GuHCl promotes two-state denaturation by preventing formation of (i.e., destabilizing) the unfolding intermediate. Continued addition of GuHCl leads to denaturation of the native state of FGF-1.

Isothermal equilibrium denaturation

The deconvolution of the CD and fluorescence data to yield fractional denatured state as a function of denaturant concentration demonstrates excellent agreement between the two methods (Fig. 6). Therefore, local unfolding near tryptophan 107 occurs simultaneously with the unfolding of secondary and tertiary features of the protein. Thus, a two-state model during isothermal equilibrium GuHCl induced unfolding of FGF-1 is supported. There is no evidence for an unfolding intermediate when FGF-1 is denatured using GuHCl under isothermal conditions at 298 K. The midpoint of the unfolding transition occurs at ~1.13 M GuHCl at this temperature. This relatively high concentration of GuHCl may therefore prevent formation of an unfolding intermediate. Thus, there is a critical range of temperature and denaturant which allows isolation of a soluble unfolding intermediate.

TABLE 2 Comparison of ΔG for DSC, CD, and fluorescence studies

Method	ΔG_0 (kJ mol^{-1})	m Value (kJ L mol^{-2})	GuHC (M) @ $\Delta G = 0$
Fluorescence	21.92 ± 0.26	−19.44 ± 0.22	1.13 ± 0.01
CD	20.76 ± 0.39	−18.67 ± 0.35	1.11 ± 0.02
DSC	21.22 ± 1.00	−18.26 ± 1.04	1.16 ± 0.05
Average	21.30 ± 0.58	−18.79 ± 0.60	1.13 ± 0.03

The DSC data are determined at the reference temperature of 298.15 K and includes data over the range of GuHCl where the reversible denaturation is two-state (i.e., 0.7–1.1 M). The values of ΔG for all studies are the extrapolated values at 0 M denaturant. Reported error is from the linear fit to the data.

Comparison of isothermal equilibrium and DSC data

For each concentration of denaturant in the DSC studies, ΔG can be calculated at the isothermal reference temperature (298 K) used in the CD and fluorescence studies. Thus, ΔG as a function of denaturant can be directly compared for the three methods. The extrapolated values for ΔG at 0 M denaturant (i.e., ΔG_0), m values, and concentrations of denaturant at $\Delta G = 0$ are listed in Table 2. Over the range of denaturant where the DSC data exhibit two-state reversible denaturation (0.7–1.1 M) there is excellent agreement among the DSC, CD, and fluorescence studies (Fig. 7). The average value of ΔG_0 (21.30 ± 0.58 kJ mol^{-1}) is less than the value (27.22 kJ mol^{-1}) reported from urea-induced denaturation of FGF-1 at pH 7.0 (Burke et al., 1993). However, this study was performed in phosphate buffer, which can bind and stabilize FGF-1 (Romero et al., 1996; Blaber et al., 1997). The temperature at which ΔG is a

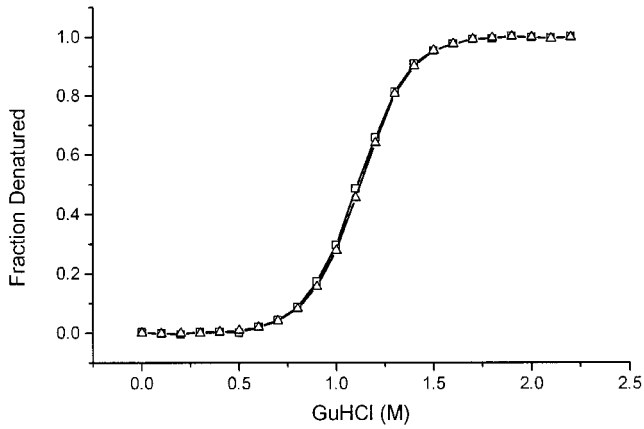

FIGURE 6 A comparison of the deconvolution of CD (*open squares*) and fluorescence data (*open triangles*) to yield a fractional denatured state as a function of GuHCl.

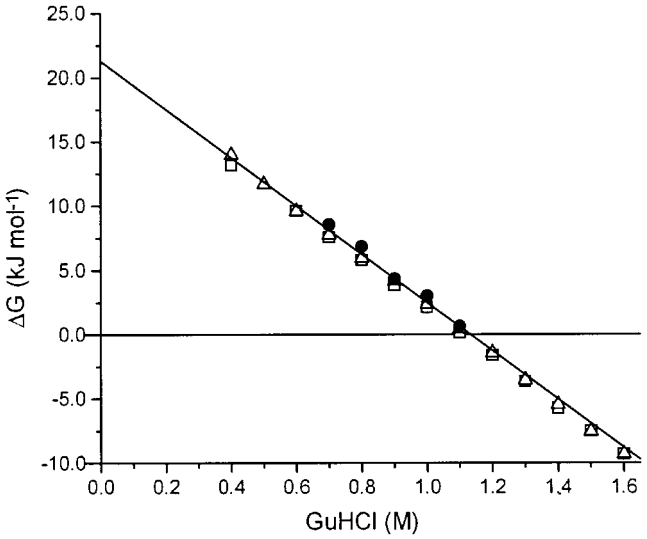

FIGURE 7 ΔG values as a function of denaturant at 298.15°C for CD (*open squares*), fluorescence (*open triangles*), and DSC data (*circles*). A linear fit to the mean value of the CD, fluorescence, and DSC data (over the range of two-state behavior; 0.7–1.1 M) is shown with a solid line.

maximum can be calculated from the derivative of the ΔG function for the DSC data, yielding a value of 289.75 ± 2.7 K (16.6°C). Linear extrapolation of T_m values to 0 M denaturant yields a surprising value of 59°C. This is significantly higher than the *apparent* T_m derived for FGF-1 under irreversible conditions (Copeland et al., 1991). Precipitation, being an irreversible process, will perturb the unfolding equilibrium, resulting in a lower apparent T_m value. Additionally, it cannot be ruled out that the native structure of FGF-1 is stabilized at low concentrations of GuHCl. However, no evidence for such initial stabilization is present in either the CD or fluorescent spectroscopic data for the isothermal GuHCl-induced denaturation (Fig. 6).

The addition of relatively low concentrations of GuHCl promotes the equilibrium two-state conditions necessary for accurate thermodynamic analysis of FGF-1. This, in turn, will allow thermodynamic studies of mutations designed to probe structure and stability relationships. Although the present study is performed under near-physiological conditions of pH, the presence of GuHCl will perturb the ΔG of unfolding in comparison to actual physiological conditions. However, the critical parameter of interest in mutant studies is typically the *difference* in the ΔG of unfolding ($\Delta\Delta G$) between mutant and wild-type protein, and not the absolute value of ΔG. Finally, the identification of conditions for the solubilization of an unfolding intermediate of FGF-1 will aid in characterization of its physical properties and structure.

The authors thank Dr. Bert van de Burgt of the Institute of Molecular Biophysics Spectroscopy Lab and Dr. Umesh Goli of the Biochemical Analysis, Synthesis and Sequencing Laboratory at FSU for expert technical assistance. The authors also thank Drs. Tim Logan, Shun-Ichi Kidokoro, Kaori Kamoshida-Chiba, John Brandts, Igor Litvinyuk, and Ms. Elena Falkovskaia for helpful discussions.

This work was supported by the Lucille P. Markey foundation and National Institutes of Health Grant GM54429-R29.

REFERENCES

Abraham, J. A., A. Mergia, J. L. Whang, A. Tumolo, J. Friedman, K. A. Hjerrild, D. Gospodarowicz, and J. C. Fiddes. 1986. Nucleotide sequence of a bovine clone encoding the angiogenic protein, basic fibroblast growth factor. *Science.* 233:545–548.

Blaber, M., D. H. Adamek, A. Popovic, and S. I. Blaber. 1997. Biophysical and structural analysis of human acidic fibroblast growth factor. Academic Press, San Diego.

Blaber, M., J. DiSalvo, and K. A. Thomas. 1996. X-ray crystal structure of human acidic fibroblast growth factor. *Biochemistry.* 35:2086–2094.

Bourque, W. T., M. Gross, and B. K. Hall. 1993. Expression of four growth factors during fracture repair. *Int. J. Dev. Biol.* 37:573–579.

Burke, C. J., D. B. Volkin, H. Mach, and C. R. Middaugh. 1993. Effects of polyanions on the unfolding of acidic fibroblast growth factor. *Biochemistry.* 32:6419–6426.

Bychkova, V. E., R. H. Pain, and O. B. Ptitsyn. 1988. The "molten globule" state is involved in the translocation of proteins across membranes? *FEBS Lett.* 238:231–234.

Colvin, J. S., B. A. Bohne, G. W. Harding, D. G. McEwen, and D. M. Ornitz. 1996. Skeletal overgrowth and deafness in mice lacking fibroblast growth factor receptor 3. *Nat. Genet.* 12:390–397.

Copeland, R. A., H. Ji, A. J. Halfpenny, R. W. Williams, K. C. Thompson, W. K. Herber, K. A. Thomas, M. W. Bruner, J. A. Ryan, D. Marquis-Omer, G. Sanyal, R. D. Sitrin, S. Yamazaki, and C. R. Middaugh. 1991. The structure of human acidic fibroblast growth factor and its interaction with heparin. *Arch. Biochem. Biophys.* 289:53–61.

Deng, X., A. Wynshaw-Boris, F. Zhou, A. Kuo, and P. Leder. 1996. Fibroblast growth factor receptor 3 is a negative regulator of bone growth. *Cell.* 84:911–921.

Eftink, M. R. 1994. The use of fluorescence methods to monitor unfolding transitions in proteins. *Biophys. J.* 66:482–501.

Fitzpatrick, L. R., A. Jakubowska, G. E. Martin, M. Davis, M. C. Jaye, and C. A. Dionne. 1992. Acidic fibroblast growth factor accelerates the healing of acetic-acid-induced gastric ulcers in rats. *Digestion.* 53: 17–27.

Freire, E., and R. L. Biltonen. 1978. Statistical mechanical deconvolution of thermal transitions in macromolecules. I. Theory and application to homogeneous systems. *Biopolymers.* 17:463–479.

Gimenez-Gallego, G., G. Conn, V. B. Hatcher, and K. A. Thomas. 1986. The complete amino acid sequence of human brain-derived acidic fibroblast growth factor. *Biochem. Biophys. Res. Commun.* 128:611–617.

Gospodarowicz, D., and J. Cheng. 1986. Heparin protects basic and acidic FGF from inactivation. *J. Cell. Physiol.* 128:475–484.

Jackson, A., S. Friedman, X. Zhan, K. A. Engleka, R. Forough, and T. Maciag. 1992. Heat shock induces the release of fibroblast growth factor 1 from NIH 3T3 cells. *Proc. Natl. Acad. Sci. USA.* 89:10691–10695.

Jaye, M., R. Howk, W. Burgess, G. A. Ricca, I.-M. Chiu, M. W. Ravera, S. J. O'Brien, W. S. Modi, T. Maciag, and W. N. Drohan. 1986. Human endothelial cell growth factor: cloning, nucleotide sequence, and chromosome localization. *Science.* 233:541–545.

Kidokoro, S.-I., H. Uedaira, and A. Wada. 1988. Determination of thermodynamic functions from scanning calorimetry data. II. For the system that includes self-dissociation/association process. *Biopolymers.* 27: 271–297.

Kidokoro, S.-I., and A. Wada. 1987. Determination of thermodynamic functions from scanning calorimetry data. *Biopolymers.* 26:213–229.

Landau, C., A. K. Jacobs, and C. C. Haudenschild. 1995. Intrapericardial basic fibroblast growth factor induces myocardial angiogenesis in a rabbit model of chronic ischemia. *Am. Heart J.* 129:924–931.

Linemeyer, D. L., L. J. Kelly, J. G. Menke, G. Gimenez-Gallego, J. DiSalvo, and K. A. Thomas. 1987. Expression in *Escherichia coli* of a chemically synthesized gene for biologically active bovine acidic fibroblast growth factor. *Biotechnology.* 5:960–965.

Linemeyer, D. L., J. G. Menke, L. J. Kelly, J. Disalvo, D. Soderman, M.-T. Schaeffer, S. Ortega, G. Gimenez-Gallego, and K. A. Thomas. 1990.

Disulfide bonds are neither required, present, nor compatible with full activity of human recombinant acidic fibroblast growth factor. *Growth Factors.* 3:287–298.

Mach, H., and C. R. Middaugh. 1995. Interaction of partially structured states of acidic fibroblast growth factor with phospholipid membranes. *Biochemistry.* 34:9913–9920.

Mach, H., D. B. Volkin, C. J. Burke, C. R. Middaugh, R. J. Linhardt, J. R. Fromm, D. Loganathan, and L. Mattsson. 1993. Nature of the interaction of heparin with acidic fibroblast growth factor. *Biochemistry.* 32: 5480–5489.

Mellin, T. N., R. J. Mennie, D. E. Cashen, J. J. Ronan, J. Capparella, M. L. James, J. DiSalvo, J. Frank, D. Linemeyer, G. Gimenez-Gallego, and K. A. Thomas. 1992. Acidic fibroblast growth factor accelerates dermal wound healing. *Growth Factors.* 7:1–14.

Nabel, E. G., Z.-Y. Yang, G. Plautz, R. Forough, X. Zhan, C. C. Haudenschild, T. Maciag, and G. J. Nabel. 1993. Recombinant fibroblast growth factor-1 promotes intimal hyperplasia and angiogenesis in arteries in vivo. *Nature.* 362:844–846.

Nakagawa, T., and Y. Oyanagi. 1980. Program system SALS for nonlinear least-squares fitting in experimental sciences. *In* Recent Developments in Statistical Inference and Data Analysis. K. Matsushita, editor. North Holland Publishing Co., Amsterdam, The Netherlands. 221–225.

Ortega, S., M. Ittmann, S. H. Tsang, M. Ehrlich, and C. Basilico. 1998. Neuronal defects and delayed wound healing in mice lacking fibroblast growth factor 2. *Proc. Natl. Acad. Sci. USA.* 95:5672–5677.

Privalov, P. L. 1979. Stability of proteins. *In* Advances in Protein Chemistry. Academic Press, New York. 167–241.

Privalov, P. L., and S. A. Potekhin. 1986. Scanning microcalorimetry in studying temperature-induced changes in proteins. *In* Methods in Enzymology. Academic Press, New York. 4–51.

Pu, L.-Q., A. D. Sniderman, R. Brassard, K. J. Lachapelle, A. M. Graham, R. Lisbona, and J. F. Symes. 1993. Enhanced revascularization of the ischemic limb by angiogenic therapy. *Circulation.* 88:208–215.

Romero, A., A. Lucena-Pineda, and G. Gimenez-Gallego. 1996. X-ray structure of native full-length human fibroblast-growth factor at 0.25-nm resolution. *Eur. J. Biochem.* 241:453–461.

Rosengart, T. K., W. V. Johnson, R. Friesel, R. Clark, and T. Maciag. 1988. Heparin protects heparin-binding growth factor-1 from proteolytic inactivation in vitro. *Biochem. Biophys. Res. Commun.* 152:432–440.

Sambrook, J., E. F. Fritsch, and T. Maniatis. 1989. Molecular Cloning: A Laboratory Manual. Cold Spring Harbor Laboratory Press, Plainview, New York.

Sanz, J. M., and G. Gimenez-Gallego. 1997. A partly folded state of acidic fibroblast growth factor at low pH. *Eur. J. Biochem.* 246:328–335.

Schlaudraff, K., B. Schumacher, B. U. v. Specht, R. Seitelberger, V. Schlosser, and R. Fasol. 1993. Growth of "new" coronary vascular structures by angiogenic growth factors. *Eur. J. Cardiothoracic Surg.* 7:637–644.

Schneider, M. D., and T. G. Parker. 1991. Cardiac growth factors. *Prog. Growth Factor Res.* 3:1–26.

Schumacher, B., P. Pecher, B. U. von Specht, and T. Stegmann. 1998. Induction of neoangiogenesis in ischemic myocardium by human growth factors: first clinical results of anew treatment of coronary heart disease. *Circulation.* 97:645–650.

Shirley, B. A. 1995. Urea and guanidine hydrochloride denaturation curves. *In* Methods in Molecular Biology. Protein Stability and Folding. B. A. Shirley, editor. Humana Press, Inc., Totowa, NJ. 177–190.

Slack, J. M. W., B. G. Darlington, J. K. Heath, and S. F. Godsave. 1987. Mesoderm induction in early *Xenopus* embryos by heparin-binding growth factors. *Nature.* 326:197–200.

Thomas, K. A., M. Rios-Candelore, G. Gimenez-Gallego, J. DiSalvo, C. Bennett, J. Rodkey, and S. Fitzpatrick. 1985. Pure brain-derived acidic fibroblast growth factor is a potent angiogenic vascular endothelial cell mitogen with sequence homology to interleukin 1. *Proc. Natl. Acad. Sci. USA.* 82:6409–6413.

Thompson, J. A., C. C. Haudenschild, K. D. Anderson, J. M. DiPietro, W. F. Anderson, and T. Maciag. 1989. Heparin-binding growth factor 1 induces the formation of organoid neovascular structures in vivo. *Proc. Natl. Acad. Sci. USA.* 86:7928–7932.

Tsai, P. K., D. B. Volkin, J. M. Dabora, K. C. Thompson, M. W. Bruner, J. O. Gress, B. Matuszewska, M. Keogan, J. V. Bondi, and C. R. Middaugh. 1993. Formulation design of acidic fibroblast growth factor. *Pharm. Res.* 10:649–659.

Unger, E. F., S. Banai, M. Shou, D. F. Lazarous, M. T. Jaklitsch, M. Scheinowitz, R. Correa, C. Klingbeil, and S. E. Epstein. 1994. Basic fibroblast growth factor enhances myocardial collateral flow in a canine model. *Am. J. Physiol.* 266:H1588–H1595.

Wiedlocha, A., I. H. Madshus, H. Mach, C. R. Middaugh, and S. Olsnes. 1992. Tight folding of acidic fibroblast growth factor prevents its translocation to the cytosol with diphtheria toxin as vector. *EMBO J.* 11: 4835–4842.

Yanagisawa-Miwa, A., Y. Uchida, F. Nakamura, T. Tomaru, H. Kido, T. Kamijo, S. Tsuneaki, K. Kaji, M. Utsuyama, C. Kurashima, and H. Ito. 1992. Salvage of infarcted myocardium by angiogenic action of basic fibroblast growth factor. *Science.* 257:1401–1403.

Zazo, M., R. M. Lozano, S. Ortega, J. Varela, R. Diaz-Orejas, J. M. Ramirez, and G. Gimenez-Gallego. 1992. High-level synthesis in *Escherichia coli* of a shortened and full-length human acidic fibroblast growth factor and purification in a form stable in aqueous solutions. *Gene.* 113:231–238.